Journal of the Korean Magnetic Resonance Society **2020**, *24*, 59-65
DOI 10.6564/JKMRS.2020.24.2.059

Nanoscale-NMR with Nitrogen Vacancy center spins in diamond

Junghyun Lee*

Center for Quantum Information, Korea Institute of Science and Technology, Seoul 02792, Republic of Korea

Received June 18, 2020; Revised June 19, 2020; Accepted June 19, 2020

Abstract Nitrogen-Vacancy (NV) center in diamond has been an emerging versatile tool for quantum sensing applications. Amongst various applications, nano-scale nuclear magnetic resonance (NMR) using a single or ensemble NV centers has demonstrated promising results, opening possibility of a single molecule NMR for its chemical structural studies or multi-nuclear spin spectroscopy for quantum information science. However, there is a key challenge, which limited the spectral resolution of NMR detection using NV centers; the interrogation duration for NV-NMR detection technique has been limited by the NV sensor spin lifetime (T_1 ~ 3ms), which is orders of magnitude shorter than the coherence times of nuclear spins in bulk liquid samples (T_2 ~ 1s) or intrinsic ^{13}C nuclear spins in diamond. Recent studies have shown that quantum memory technique or synchronized readout detection technique can further narrow down the spectral linewidth of NMR signal. In this short review paper, we overview basic concepts of nanoscale NMR using NV centers, and introduce further developments in high spectral resolution NV NMR studies.

Keywords NV center, quantum sensing, nanoscale-NMR, synchronized readout

Introduction

Recent studies have shown that spin defects in solid-state materials are promising candidate for quantum sensing applications such as sensing magnetic field,[1-3,5] electric field,[4] and even a dark matter.[6] Among different types of spin defects, the Nitrogen-Vacancy (NV) color center in diamond has many advantages due to its (i) easy optical initialization with green laser light (ii) easy control of spin states via applying resonant microwave signals and (iii) operation under ambient conditions.

NV center is a spin 1 system. Under optical illumination of 532 nm, NV center undergoes spin-state-preserving transitions between the electronic ground ($^3A_2$) and excited states (^3E), and emits fluorescence in 600 to 800 nm band with a life

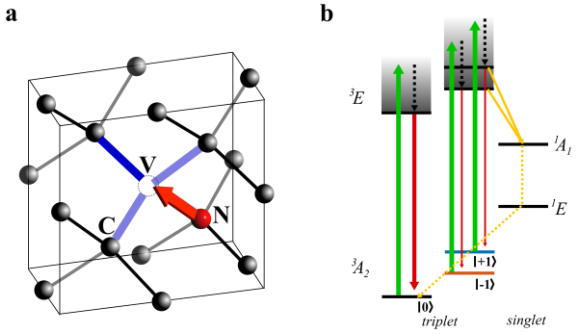

Figure 1 (a) The structure of diamond crystal with an NV center. NV center consists of a substitutional nitrogen atom (N) adjacent to a vacancy (V) in the diamond lattice. The direction along the nitrogen atom and the vacancy (red arrow) defines the quantization axis of the NV center. Blue rod indicates four possible orientations for different class of NV centers. B) NV center energy level diagram. From J. Lee *et al*., 2018

* Correspondence to: **Junghyun Lee,** Center for Quantum Information, Korea Institute of Science and Technology, Seoul 02792, Republic of Korea, E-mail: jh_lee@kist.re.kr

time of ~ 13 ns, and zero phonon line lies at around 637nm. There also exists a non-radiative decay path from $|m_s = \pm1\rangle$ excited states to $|m_s = 0\rangle$ ground state via metastable singlet states ($^1A_1$ and ^1E) with lifetime of ~ 300 ns.[7] Due to leakage to a singlet state, when green laser continuously illuminates NVs in diamond, the NV spin state is polarized into $|m_s = 0\rangle$ state.[8] With similar mechanism, when the NV spin is at $|m_s = \pm1\rangle$ state, we measure diminished fluorescence, and this is how NV spin state is readout optically. NV spin state can be controlled via resonant microwave signal, which induces state transition between $|m_s = 0\rangle$ and $|m_s = +1\rangle$ or $|m_s = -1\rangle$. Resonant frequencies are determined by optically detected magnetic resonance (ODMR)[9] where resonances are Zeeman energy split by external bias magnetic field, centered at the zero-field splitting of ~2.87GHz. NV center is an atomic scale spin sensor, which has shown very promising results in DC and AC magnetic field sensing. One major advantage over other quantum sensing tools such as superconducting quantum interface device (SQUID) [10] or atomic vapor cell based sensors[11] is its proximity to a target sample. Recent improvements in detectable magnetic field sensitivity,[12] field range,[13] spatial[14] and spectral resolution[15-17] has shown that NV spin sensor is one of the leading magnetic field sensing platforms. Among variety of NV spin's sensing applications, in this review paper, we introduce short overview of NV based NMR studies; Basic concept of NV NMR detection, synchronized readout protocol for high spectral resolution NV NMR, high resolution detection of real NMR sample with NV, and hyperpolarization combined with high spectral resolution NV NMR to detect chemical shifts in dilute sample with picoliter detection volume.

NV-detected NMR protocol

Key advantage of NV-NMR comes in when we maximize the sample detection volume from which the AC magnetic field NMR signal is generated. Shallower the NV sensor spin is, stronger the signal from larger detection volume is. Such shallow NV diamond sample can be created by optimizing the nitrogen ion implantation energy.[18] Few keV of implantation energy is used to create few nm deep NV spin. To detect NMR signal using NV sensor spin, we use conventional AC-magnetometry techniques, such as CPMG (Carr-Purcell-Meiboom -Gill) pulse sequence or XY pulse sequence.[19,20] These dynamical decoupling sequences consist of consecutive π pulses, providing an AC signal filter, which makes spin only to accumulate net phase at a specific oscillating NMR signal frequency. Most commonly used n-pulsed CPMG is an extension of

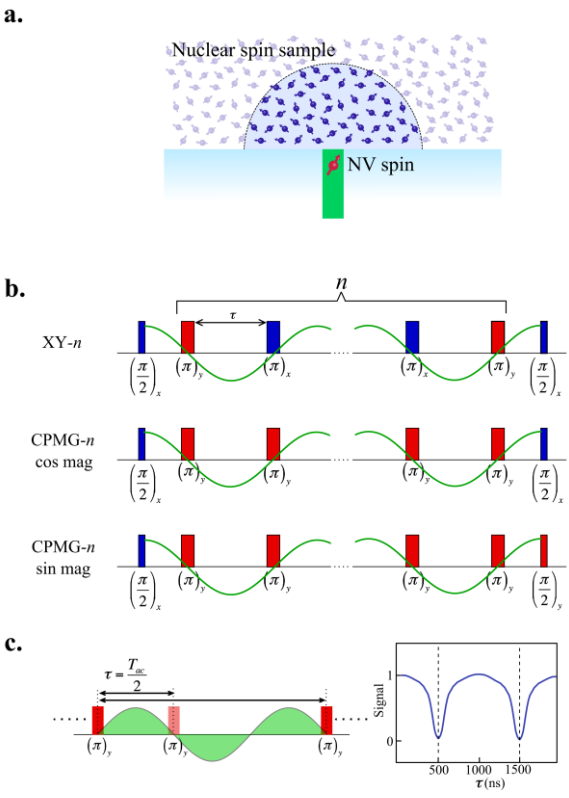

Figure 2 (a) NV NMR schematics. Red spin indicates NV sensor spin in diamond, and blue hemisphere with blue spins indicates detectable nuclear spin sample volume. (b) XYn, CPMGn cosine and sine AC magnetometry pulse seuqnces. c, Green oscillation indicates external AC magnetic field, and when π pulse spacing satisfies $\tau = (2n + 1)T_{ac}/2$, we can see signal (spin coherence) collapse. From J. Lee *et al.*, 2018.

Hahn-echo sequence where there are n-repeated, equally spaced refocusing π pulses between two Hadamard gate rotation π/2 pulses, which prepare NV spin into superposition state between $|m_s = 0\rangle$ and $|m_s = -1\rangle$ or $|m_s = +1\rangle$. Moreover, by modulating the phase of the MW signal, the spin rotation axis of π pulse train is set to be 90 degree rotated from the first π/2 pulse. Switching rotation axis and having an even number of π pulses compensate possible pulses errors, which could accumulate along one spin rotation axis. To minimize pulse errors, XYn pulse sequence, which has alternating π rotation around X and Y axis is widely adopted for more robust AC-magnetometry. Depending on the phase of the last π/2 pulse, there are two types of AC-magnetometry protocols; when the last π/2 pulse has the same phase as the initial π/2 pulse, it is called AC cosine magnetometry and when the last π/2 pulse has 90 degree out of phase from the initial π/2 pulse, it is called AC sine magnetometry. Each magnetometry protocol has different response to an external AC magnetic field. AC cosine magnetometry pulse sequences have a *quadratic* dependence of the final NV spin population on the magnetic field signal in order to rectify the zero-mean noise component and sense its variance. On the other hand, in AC sine magnetometry, final NV spin population is *linearly* dependent on the amplitude of the total oscillating magnetic field signal.

NV-NMR signal detection is done by measuring the NV spin coherence while sweeping the time interval τ between π pulses. Let's assume there is an oscillating coherent magnetic field, $b(t) = b_{ac} \sin(2\pi f_{ac} + \varphi)$, with frequency f_{ac} (period $T_{ac} = 1/f_{ac}$). Free precession time between π pulses in CPMGn or XYn pulse sequence, τ, is varied to detect that oscillating magnetic field. Once τ matches to $T_{ac}/2$, in which π pulses are placed at every zeros of $b(t)$ field, at each τ duration, NV spin gains phase due to external $b(t)$ field. This phase is accumulated throughout whole CPMGn or XYn pulse sequence as NV spin is flipped by π pulses whenever $b(t)$ field flips its sign. This appears as dips in spin coherence plots (Figure 2c). Furthermore, phase accumulation happens in the following harmonics, $\tau = (2n+1)T_{ac}/2$.

Early work in nanoscale NMR using NV successfully detected different nuclear species in non-uniform liquid sample.[22-25] NV-NMR signal linewidth broadening happens under two main circumstances. First, the nuclear spin sample itself can cause broadening; Short inhomogeneous dephasing time T_2^*(or T_2) when refocusing pulse is used, limiting NV-NMR signal linewidth by $1/\pi T_2^*$ and nuclear spin diffusion happening at the border of detection volume. Secondly, NV sensor spin coherence time T_2 itself can limit the signal linewidth since there is limit in extending the spin coherence time via dynamical decoupling. With ensemble NV sample, normal NV-NMR detection scheme using CPMGn or XYn pulse sequences has signal linewidth of ~kHz range. One way to overcome short NV spin sensor lifetime issue is to further extend it by using nearby nuclear spin memory.[15,16] Intrinsic nuclear spin, such as ^{13}C in diamond has much longer spin lifetime compared to NV spin and through correlation measurement on NV-nuclear spin hybrid system, we expect to narrow NV-NMR signal linewidth. Alternative method to extend effective NV spin lifetime is to use Synchronized Readout scheme.[17]

High spectral resolution NV-NMR SR protocol

In this section, we review recently developed high spectral resolution NV-NMR scheme, called Synchronized Readout (SR), which successfully demonstrated ~Hz range signal linewidth. The idea of the SR-NMR signal detection protocol is based on signal mixing between an external oscillating magnetic field - nuclear Larmor oscillation signal or other AC magnetic signal - and periodic readout of sensor spin magnetometry response, all synchronized to an external clock. Each block of sensor spin response readout consists of an NV AC magnetometry pulse sequence and optical readout/initialization pulses. This block of identical pulse sequence is equidistantly positioned with the multiples of $1/f_0$. (Here, f_0 is the center frequency of the AC magnetometry spectral response)

Given that the external oscillating magnetic field has frequency of f_{ac}, if $f_{ac} = f_0$, then the NV fluorescence readout from each block will have the same signal amplitude, assuming that external field amplitude

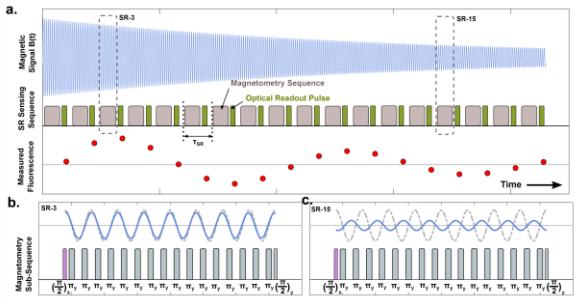

Figure 3 (a) Numerical simulation of SR detection of a free induction decay (FID) signal, *b(t)* (blue). The SR sequence consists of interspersed blocks of identical NV magnetometry sub-sequences (gray boxes) and optical NV spin state readouts (green boxes). SR readouts oscillates at frequency $\Delta f = |f_{ac} - f_0|$, because the FID signal phase advances incrementally relative to the magnetometry sub-sequence. (b) Detail of calculated magnetic signal and magnetometry subsequence at the third SR iteration (denoted SR-3) then the signal (blue line) is nearly in phase. Detected fluoresce is maximum because the FID is in phase. c, Magnetic signal and magnetometry subsequence at SR-15 when The signal has advanced and is now ~ 180 degree out of phase. This gives rise to a detected fluorescence minimum at SR-15. From D. Glenn *et al*., 2018.

does not decay. However, if $f_{ac} \neq f_0$, then the NV fluorescence signal will oscillate at $\Delta f = |f_{ac} - f_0|$. Performing *Fast Fourier Transform* on the time series NV fluorescence signal, Δf, which is the effective AC signal, can be measured. To check the parity of Δf, we can always modify f_0 and follow the trend of Δf. For the maximum contrast in SR NV fluorescence signal oscillation, NV AC magnetometry pulse is tuned with the external oscillating magnetic field frequency f_{ac}. Since NV sensor spin is repeatedly initialized and readout, actively detecting external AC signal, linewidth of NMR signal no longer depends on the NV spin lifetime.

Demonstration of high spectral resolution

NV-NMR via SR

Synchronized readout requires careful external clock synced lock-in detection. Any jittering of clock during the measurement can cause unwanted broadening in signal linewidth. SR may be applied to signals with random phases, providing spectral resolution proportional to the inverse correlation time of the signal τ_c^{-1}, by incoherent averaging using periodogram techniques,[26] which is called incoherently averaged synchronized readout (IASR). On the other hand, When the oscillating external magnetic fields initial phase is locked to SR sequence, we can coherently average the signal, which we call coherently averaged synchronized readout (CASR).

Proof of principle SR measurement of artificially generated AC field through coil near the diamond shows ~mHz of signal linewidth. Both single and ensemble NV spin measurements are capable for SR measurement, yet the signal-to-noise ratio (SNR) is much better in ensemble measurement.

For successful NMR using a single-NV synchronized readout scheme, the requirement of weak sample-sensor coupling (due to the back-action to nuclear spins when NV spins are repeatedly readout), the presence of fast spin diffusion in nanometer-scale, and the imperfect spin state readout of single NV experiments,[27] all imposes a significant technical

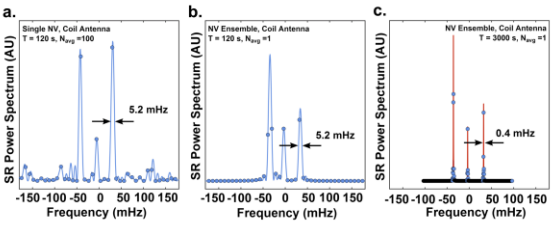

Figure 4 (**a**) Power spectrum of SR signal obtained with a single-NV in a confocal microscope. Total experiment duration T = 112.5. The observed spectral width was 5.2 mHz (FWHM). (b) Power spectrum of SR signal obtained with NV ensemble with same time duration. The observed spectral width was again 5.2 mHz. **c**, Power spectrum of SR signal obtained with NV ensemble with T = 3000s. The observed spectral width was 0.4 mHz (FWHM), broader than the Fourier limit. From D. Glenn *et al*., 2018.

challenge.

Next, applying ensemble NV SR to real NMR sample shows NV-detected NMR signal spectral resolution approaching ~ 1 Hz. An ensemble NV sensor enables: (i) probing micrometer-scale measurement volumes to obtain a signal mainly from the thermal spin polarization, which is not limited by diffusion; and (ii) employing a CASR protocol to coherently sense NMR signals for an arbitrary duration (up to ~

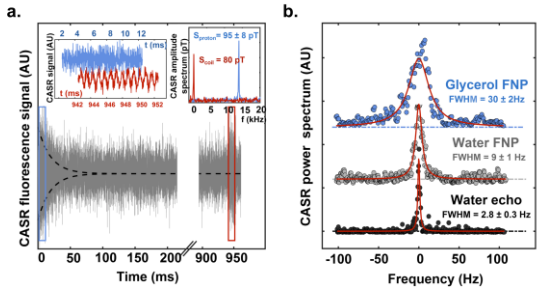

Figure 5 (a) CASR time-series signal (gray trace) produced by NMR free nuclear precession (FNP) of glycerol proton spins above the diamond, with decay time $T_2^* = 10 \pm 1$ ms (dashed line). Total signal averaging time was 7.2 × 104 s. (b) Power spectra of measured CASR FNP from protons in glycerol (blue circles) and pure water (gray circles), as well as CASR-spin-echo from pure water (black circles). Spectral resolution obtained with CASR-spin-echo approached 2.8 ± 0.3 Hz (FWHM). Signal averaging time was 3.9 × 104 s for water spin echo. From D. Glenn *et al*., 2018.

103s), which gives better SNR than that of single NV spin measurement. Recently developed NV-NMR ensemble instrument has a sensor volume that consists of the overlap region between a 13µm NV-doped layer (NV concentration [NV] ≈ 3×10^{17} cm^{-3}) at the diamond surface, and a 20 µm diameter optical excitation beam. Number of NV spins involved in sensing goes up to ~ 1.2 × 10^9, and measured ensemble sensor magnetic field sensitivity is at ηB = 30 pT $Hz^{-1/2}$. An important remark to make is that in SR, detectable magnetic field sensitivity is independent of the total measurement time; no trade-off between high sensitivity and high spectral resolution. Yet, the challenge of short signal detectable times from nanoscale liquid-state NMR samples due to molecular spin diffusion is not solved, limiting the advantages of a spectrally resolvable nanoscale sensor. Geometrically confining these nuclear spin samples from diffusion has shown some promising results.[28]

Combination of DNP with SR to maximize SNR

To overcome limited SNR due to dependence on thermal polarization of nuclear spins, recent study has shown improved SNR via combining Overhauser dynamic nuclear polarization (DNP) with high resolution SR NMR spectroscopy.[29] Initially nuclear spins are hyperpolarized using electronic spin drive. Polarization transfer happens through stochastic interactions between electronic spins and nuclear spins.[30] After ~300ms of continuous pumping of polarization from electronic spin to nuclear spin via DNP, CASR scheme is performed to detect NMR signal, showing ~×230 increase in signal magnitude compared to no DNP case.

Conclusion

In this review, we introduced a few milestone achievements towards high performance nanoscale NV NMR. First NV NMR adopted conventional NMR technique, and successfully detected NMR signal from different nuclear spin samples. Then, we developed synchronized readout technique to reduce NMR signal linewidth beyond NV sensor spin lifetime. To overcome low SNR issue, SR technique is combined with nuclear spin hyperpolarization in order to detect NMR signal in a dilute sample. These consecutive results open a door to high-resolution spectroscopy on a small molecules in dilute solutions, To overcome these challenges, large ensemble of NV spins is used. Ensemble SR-NMR demo shows that NV spin sensor itself has sufficient spectral resolution for identification of molecular NMR signatures such as J-couplings and chemical shifts, with femtomole sensitivity and variety of

applications are possible from picoliter scale in drug studies, catalysis research, and even a single-cell studies.

Acknowledgements

This work was supported by the National Research Foundation of Korea(NRF), funded by the Ministry of Science and ICT (2019M3E4A107866011) and KIST institutional research program (2E29580).

References

1. J. M. Taylor, P. Cappellaro, L. Childress, L. Jiang, D. Budker, P. R. Hemmer, A. Yacoby, R. L. Walsworth, and M. D. Lukin. *Nat. Phys.* **4**, 810 (2008)
2. D. Le Sage, K. Arai, D. R. Glenn, S. J. DeVience, L. M. Pham, L. Rahn-Lee, M. D. Lukin, A. Yacoby, A. Komeili, and R. L. Walsworth. *Nature* **496**, 486 (2013)
3. M. S. Grinolds, S. Hong, P. Maletinsky, L. Luan, M. D. Lukin, R. L. Walsworth, and A. Yacoby. *Nat. Phys.* **9**, 215 (2013)
4. F. Dolde, H. Fedder, M. W. Doherty, T. Nbauer, F. Rempp, G. Balasubramanian, T. Wolf, F. Reinhard, L. C. L. Hollenberg, F. Jelezko, and J. Wrachtrup. *Nat. Phys.* **7**, 459 (2011)
5. Matthew J. Turner, Nicholas Langellier, Rachel Bainbridge, Dan Walters, Srujan Meesala, Thomas M. Babinec, Pauli Kehayias, Amir Yacoby, Evelyn Hu, Marko Lončar, Ronald L. Walsworth, Edlyn V. Levine. arXiv **03707** (2020)
6. S. Rajendran, N. Zobrist, A. O. Sushkov, R. L. Walsworth, and M. D. Lukin. *Phys. Rev. D* **96**, 035009 (2017)
7. L. Robledo, H. Bernien, T. van der Sar, and R. Hanson. *New J. Phys.* **13,** 025013 (2011)
8. L. Childress. PhD thesis, *Harvard University* (2006)
9. H. Lee, J. Shim**,** *J. Kor. Magn. Reson. Soc.* **22**, 40 (2018)
10. L. P. Lee, K. Char, M. S. Colclough, and G. Zaharchuk, *App. Phys. Lett*. **59**, 3051 (1991)
11. P. D. D. Schwindt, S. Knappe, V. Shah, L. Hollberg, and J. Kitching, *App. Phys. Lett*. **85**, 6409 (2004)
12. J. F. Barry, J. M. Schloss, E. Bauch, M. J. Turner, C. A. Hart, L. M. Pahm, and R. L. Walsworth, *Rev. Mod. Phys.* **92**, 015004 (2020)
13. K. Arai, J. Lee, C. Belthangady, D. R. Glenn, H. Zhang, and R. L. Walsworth, *Nat. Comm.* **9**, 4996 (2018)
14. K. Arai, C. Belthangady, H. Zhang, N. Bar-Gill, S. J. DeVience, P. Cappellaro, A. Yacoby, R. L. Walsworth, *Nat. Nanotechnol.* **10**, 859 (2015)
15. S. Zaiser, T. Rendler, I. Jakabi, T. Wolf, S. Lee, S. Wagner, V. Bergholm, T. Schute-Herbruggen, P. Neumann, and J. Wrachtrup, *Nat. Comm.* **7**, 12279 (2016)
16. N. Aslam, M. Pfender, P. Neumann, R. Reuter, A. Zappe, F. Oliveira, A. Denisenko, H. Sumiya, S. Onoda, J. Isoya, and J. Wrachtrup. *Science* **10**, 1126 (2017)
17. D. R. Glenn, D. B. Bucher, J. Lee, M. D. Lukin, H. Park and R. L. Walsworth, *Nature* **555**, 351 (2018)
18. S. Oh, *J. Kor. Magn. Reson. Soc.* **23**, 73 (2019)
19. S. Meiboom and D. Gill. *Rev. Sci. Instrum.* **29**, 688 (1958)
20. H. Y. Carr and E. M. Purcell. *Phys. Rev.* **94**, 630 (1954)
21. J. Lee, PhD thesis, *Massachusetts Institute of Technology* (2018)
22. L. M. Pham, S. J. DeVience, F. Casola, I. Lovchinsky, A. O. Sushkov, E. Bersin, J. Lee, E. Urbach, P.

Cappellaro, H. Park, A. Yacoby, M. Lukin and R. L. Walsworth. *Phys. Rev. B* **93**, 045425 (2016)
23. S. J. DeViencea, L. M. Pham, I. Lovchinsky, A. O. Sushkov, N. Bar-Gill, C. Belthangady, F. Casola, M. Corbett, H. Zhang, M. Lukin, H. Park, A. Yacoby, and R. L. Walsworth. *Nat. Nanotechnol.* **10**, 129 (2015)
24. H. J. Mamin, M. Kim, M. H. Sherwood, C. T. Rettner, K. Ohno, D. D. Awschalom, and D. Rugar. *Science*, **339**, 557 (2013)
25. T. Staudacher, F. Shi, S. Pezzagna, J. Meijer, J. Du, C. A. Meriles, F. Reinhard, and J. Wrachtrup. *Science*, **339**, 561 (2013)
26. S. M. Alessio. Digital signal processing and spectral analysis for scientists: concepts and applications. *Springer* (2016)
27. M. W. Doherty, N. B. Manson, P. Delaney, F. Jelezko, J. Wrachtrup, and L. C. L. Hollenberg. *Phys. Rep.* **528**, 1 (2013)
28. P. Kehayias, A. Jarmola, N. Mosavian, I. Fescenko, F. M. Benito, A. Laraoui, J. Smits, L. Bougas, D. Budker, A. Neumann, S. R. J. Brueck, and V. M. Acosta. *Nat. Comm.* **8**, 188 (2017)
29. D. B. Bucher, D. R. Glenn, H. Park, M. D. Lukin, R. L. Walsworth. *Phys. Rev. X* **10**, 021053 (2020)
30. A. W. Overhauser, Polarization of Nuclei in Metals, *Phys. Rev.* **92**, 411 (1953)